Constraining PDFs with J/ψ & Υ inclusive photoproduction

Yelyzaveta Yedelkina

work done in collaboration with Carlo Flore, Jean-Philippe Lansberg, Hua-Sheng Shao, Alice Colpani Serri, Yu Feng, Melih A. Ozcelik in IJCLab (Orsay)

Kickoff meeting - GDR-QCD / WG1,
Quarkonium & QCD meeting, Aussois, June 23, 2021

Part I

Introducing J/ψ & Υ photoproduction

Introduction: inclusive $J/\psi(\Upsilon)$ inclusive photoproduction

C.-H. Chang, NPB172, 425 (1980); R. Baier & R. Rückl Z. Phys. C 19, 251(1983);

In this work we discuss **inclusive $J/\psi(\Upsilon)$ photoproduction**:

Introduction: inclusive $J/\psi(\Upsilon)$ inclusive photoproduction

C.-H. Chang, NPB172, 425 (1980); R. Baier & R. Rückl Z. Phys. C 19, 251(1983);

In this work we discuss **inclusive $J/\psi(\Upsilon)$ photoproduction**:

- as a reminder, J/ψ (Υ) is a $c\bar{c}$ $(b\bar{b})$ bound state with $J = 1,\ L = 0,\ S = 1$; vector particle

Introduction: inclusive $J/\psi(\Upsilon)$ inclusive photoproduction

C.-H. Chang, NPB172, 425 (1980); R. Baier & R. Rückl Z. Phys. C 19, 251(1983);

In this work we discuss **inclusive $J/\psi(\Upsilon)$ photoproduction**:

- as a reminder, J/ψ (Υ) is a $c\bar{c}$ ($b\bar{b}$) bound state with $J = 1,\ L = 0,\ S = 1$; vector particle
- inclusive photoproduction:

$$\gamma + p \to J/\psi + X. \tag{1}$$

Introduction: inclusive $J/\psi(\Upsilon)$ inclusive photoproduction

C.-H. Chang, NPB172, 425 (1980); R. Baier & R. Rückl Z. Phys. C 19, 251(1983);

In this work we discuss **inclusive $J/\psi(\Upsilon)$ photoproduction**:

- as a reminder, J/ψ (Υ) is a $c\bar{c}$ ($b\bar{b}$) bound state with $J = 1,\ L = 0,\ S = 1$; vector particle
- inclusive photoproduction:

$$\gamma + p \to J/\psi + X. \tag{1}$$

- We will discuss the photoproduction at high & low P_T.

Introduction: inclusive $J/\psi(\Upsilon)$ inclusive photoproduction

C.-H. Chang, NPB172, 425 (1980); R. Baier & R. Rückl Z. Phys. C 19, 251(1983);

In this work we discuss **inclusive $J/\psi(\Upsilon)$ photoproduction**:

- as a reminder, J/ψ (Υ) is a $c\bar{c}$ ($b\bar{b}$) bound state with $J = 1,\ L = 0,\ S = 1$; vector particle
- inclusive photoproduction:

$$\gamma + p \to J/\psi + X. \tag{1}$$

- We will discuss the photoproduction at high & low P_T.
- We do not consider in this work:
  - hadroproduction (pp collisions);
  - resolved-photon contributions (low z);
  - UPC (pA and AA collisions);
  - diffractive (large z).

Introduction: inclusive $J/\psi(\Upsilon)$ inclusive photoproduction

C.-H. Chang, NPB172, 425 (1980); R. Baier & R. Rückl Z. Phys. C 19, 251(1983);

In this work we discuss **inclusive $J/\psi(\Upsilon)$ photoproduction**:

- as a reminder, J/ψ (Υ) is a $c\bar{c}$ $(b\bar{b})$ bound state with $J = 1,\ L = 0,\ S = 1$; vector particle
- inclusive photoproduction:

$$\gamma + p \to J/\psi + X. \tag{1}$$

- We will discuss the photoproduction at high & low P_T.
- We do not consider in this work:
  - hadroproduction (pp collisions);
  - resolved-photon contributions (low z);
  - UPC (pA and AA collisions);
  - diffractive (large z).
- Inclusive photoproduction allows one to probe PDFs.

Basic pQCD approach: the Colour Singlet Model (CSM)

C.-H. Chang, NPB172, 425 (1980); R. Baier & R. Rückl Z. Phys. C 19, 251(1983);

CSM: we use the Taylor series expansion of the amplitude in the $Q\overline{Q}$ relative momentum to the first non-vanishing term.

Basic pQCD approach: the Colour Singlet Model (CSM)

C.-H. Chang, NPB172, 425 (1980); R. Baier & R. Rückl Z. Phys. C 19, 251(1983);

CSM: we use the Taylor series expansion of the amplitude in the $Q\overline{Q}$ relative momentum to the first non-vanishing term.

One supposes **factorisation**:

1. **collinear**, in which the hadronic cross section can be written as the convolution of the PDFs with the partonic cross section;

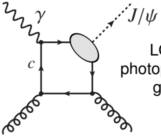

LO J/ψ photoproduction graph

NB: The quark and anti-quark attached to the ellipsis are taken as on-shell and their relative velocity v is set to zero.

Basic pQCD approach: the Colour Singlet Model (CSM)

C.-H. Chang, NPB172, 425 (1980); R. Baier & R. Rückl Z. Phys. C 19, 251(1983);

CSM: we use the Taylor series expansion of the amplitude in the $Q\overline{Q}$ relative momentum to the first non-vanishing term.

One supposes **factorisation**:

1. **collinear**, in which the hadronic cross section can be written as the convolution of the PDFs with the partonic cross section;
2. **between the hard part** (a perturbative amplitude) and **the soft part** (a non-perturbative matrix element, which describes hadronisation):

- Perturbative creation of 2 quarks Q and $\bar{Q}$

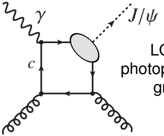

LO J/ψ photoproduction graph

NB: The quark and anti-quark attached to the ellipsis are taken as on-shell and their relative velocity v is set to zero.

Basic pQCD approach: the Colour Singlet Model (CSM)

C.-H. Chang, NPB172, 425 (1980); R. Baier & R. Rückl Z. Phys. C 19, 251(1983);

CSM: we use the Taylor series expansion of the amplitude in the $Q\overline{Q}$ relative momentum to the first non-vanishing term.

One supposes **factorisation**:

1. **collinear**, in which the hadronic cross section can be written as the convolution of the PDFs with the partonic cross section;
2. **between the hard part** (a perturbative amplitude) and **the soft part** (a non-perturbative matrix element, which describes hadronisation):

- Perturbative creation of 2 quarks Q and $\bar{Q}$ BUT
  - on-shell ($\times$)
  - in a colour singlet state
  - with a vanishing relative momentum
  - in a $^3S_1$ state (for J/ψ, ψ' and Υ)
- Non-perturbative binding of quarks

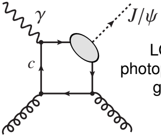

LO J/ψ photoproduction graph

NB: The quark and anti-quark attached to the ellipsis are taken as on-shell and their relative velocity v is set to zero.

Basic pQCD approach: the Colour Singlet Model (CSM)

C.-H. Chang, NPB172, 425 (1980); R. Baier & R. Rückl Z. Phys. C 19, 251(1983);

CSM: we use the Taylor series expansion of the amplitude in the $Q\overline{Q}$ relative momentum to the first non-vanishing term.

One supposes **factorisation**:

1. **collinear**, in which the hadronic cross section can be written as the convolution of the PDFs with the partonic cross section;
2. **between the hard part** (a perturbative amplitude) and **the soft part** (a non-perturbative matrix element, which describes hadronisation):

- Perturbative creation of 2 quarks Q and $\bar{Q}$ BUT
  - on-shell ($\times$)
  - in a colour singlet state
  - with a vanishing relative momentum
  - in a $^3S_1$ state (for J/ψ, ψ' and Υ)

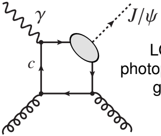

LO J/ψ photoproduction graph

- Non-perturbative binding of quarks $\rightarrow$ Schrödinger wave function

NB: The quark and anti-quark attached to the ellipsis are taken as on-shell and their relative velocity v is set to zero.

General structure of NLO corrections

Singularities at NLO [and how they are removed]:

NB1: At large P_T $(J/\psi + c)$ & QED contributions can also be important.

General structure of NLO corrections

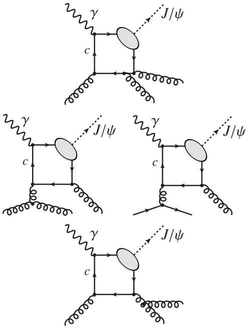

Singularities at NLO [and how they are removed]:

- Real emission
  - Infrared divergences: Soft [cancelled by loop Infrared contribution]
  - Infrared divergences: Collinear

NB1: At large P_T $(J/\psi + c)$ & QED contributions can also be important.

General structure of NLO corrections

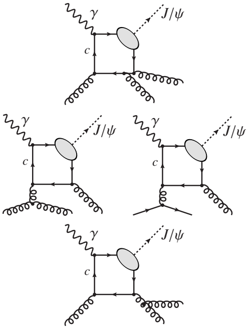

Singularities at NLO [and how they are removed]:

- Real emission
  - Infrared divergences: Soft [cancelled by loop Infrared contribution]
  - Infrared divergences: Collinear

NB1: At large P_T $(J/\psi + c)$ & QED contributions can also be important.

General structure of NLO corrections

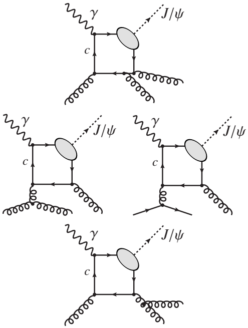

Singularities at NLO [and how they are removed]:

- Real emission
  - Infrared divergences: Soft [cancelled by loop Infrared contribution]
  - Infrared divergences: Collinear
    - ★ initial emission [subtracted by AP-CT in the factorised PDFs]
    - ★ final emission [phase-space integration (the KLN theorem)]

NB1: At large P_T $(J/\psi + c)$ & QED contributions can also be important.

General structure of NLO corrections

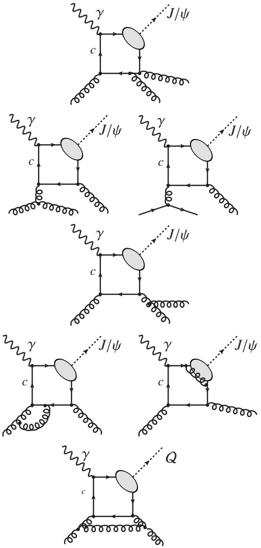

Singularities at NLO [and how they are removed]:

- Real emission
  - Infrared divergences: Soft [cancelled by loop Infrared contribution]
  - Infrared divergences: Collinear
    - ★ initial emission [subtracted by AP-CT in the factorised PDFs]
    - ★ final emission [phase-space integration (the KLN theorem)]
- Virtual (loop) contribution

NB1: At large P_T $(J/\psi + c)$ & QED contributions can also be important.

General structure of NLO corrections

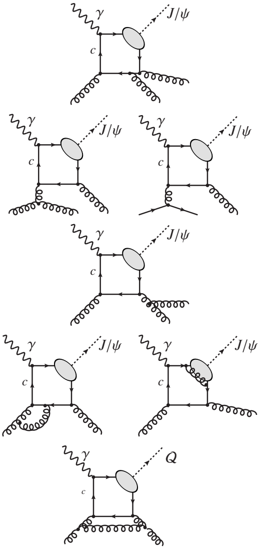

Singularities at NLO [and how they are removed]:

- Real emission
  - Infrared divergences: Soft [cancelled by loop Infrared contribution]
  - Infrared divergences: Collinear
    - ★ initial emission [subtracted by AP-CT in the factorised PDFs]
    - ★ final emission [phase-space integration (the KLN theorem)]
- Virtual (loop) contribution
  - Ultraviolet divergences: [removed by renormalisation]
  - Infrared divergences: [cancelled by real Infrared contribution]

NB1: At large P_T $(J/\psi + c)$ & QED contributions can also be important.

Part II

Photoproduction at mid and high P_T at HERA

Different contributions in the CSM up to NLO

C. Flore, J.P. Lansberg, H.S. Shao, YY, PLB 811 (2020) 135926

Different contributions in the CSM up to NLO

C. Flore, J.P. Lansberg, H.S. Shao, YY, PLB 811 (2020) 135926

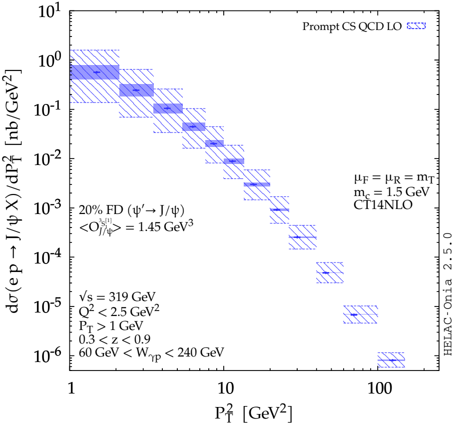

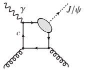

$\gamma + g \to \psi + g$ @ $\alpha\alpha_s^2$

Notes:
All the computations were done with HELAC-ONIA. The scale and mass uncertainties are shown by the hatched and solid bands. **H.S. Shao, CPC198 (2016) 238**; See also `https://nloaccess.in2p3.fr`

[The quark and antiquark attached to the ellipsis are taken as on-shell and their relative velocity v is set to zero.]

Different contributions in the CSM up to NLO

C. Flore, J.P. Lansberg, H.S. Shao, YY, PLB 811 (2020) 135926

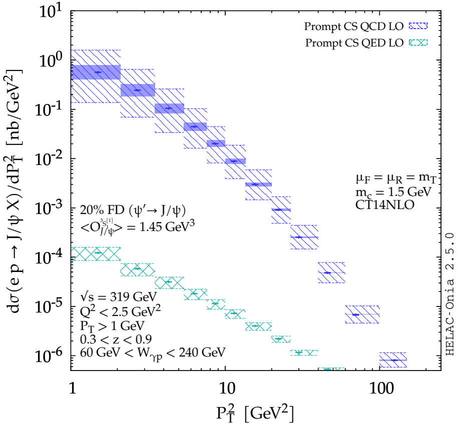

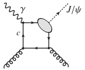

$\gamma + g \to \psi + g$ @ $\alpha\alpha_s^2$

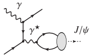

$\gamma + q \to \psi + q$ @ α^3

Notes:
All the computations were done with HELAC-ONIA. The scale and mass uncertainties are shown by the hatched and solid bands. **H.S. Shao, CPC198 (2016) 238**; See also `https://nloaccess.in2p3.fr`

[The quark and antiquark attached to the ellipsis are taken as on-shell and their relative velocity v is set to zero.]

Different contributions in the CSM up to NLO

C. Flore, J.P. Lansberg, H.S. Shao, YY, PLB 811 (2020) 135926

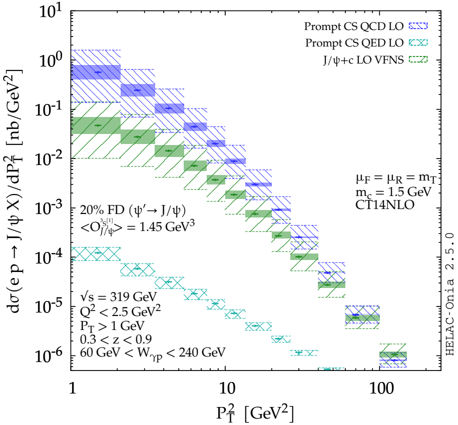

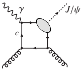

$\gamma + g \to \psi + g \,@\, \alpha\alpha_s^2$

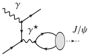

$\gamma + q \to \psi + q \,@\, \alpha^3$

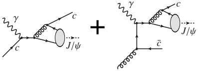

$$\left\{ \begin{array}{l} \gamma+c\to\psi+c \,@\, \alpha\alpha_s^2 \text{ w. 4 Flavour Scheme} \\ \gamma+g\to\psi+c+\bar{c} \,@\, \alpha\alpha_s^3 \text{ w. 3 Flavour Scheme} \end{array} \right.$$

Notes:
All the computations were done with HELAC-ONIA. The scale and mass uncertainties are shown by the hatched and solid bands. **H.S. Shao, CPC198 (2016) 238**; See also `https://nloaccess.in2p3.fr`

[The quark and antiquark attached to the ellipsis are taken as on-shell and their relative velocity v is set to zero.]

Different contributions in the CSM up to NLO

C. Flore, J.P. Lansberg, H.S. Shao, YY, PLB 811 (2020) 135926

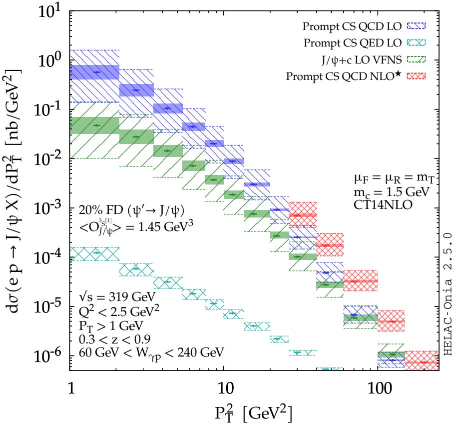

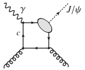

$\gamma + g \to \psi + g \,@\, \alpha\alpha_s^2$

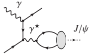

$\gamma + q \to \psi + q \,@\, \alpha^3$

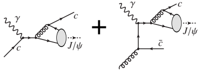

$\gamma + c \to \psi + c \,@\, \alpha\alpha_s^2$ w. 4 Flavour Scheme

$\gamma + g \to \psi + c + \bar{c} \,@\, \alpha\alpha_s^3$ w. 3 Flavour Scheme

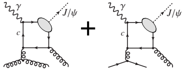

$\gamma + g \to \psi + g + g \,@\, \alpha\alpha_s^3$

$\gamma + q \to \psi + g + q \,@\, \alpha\alpha_s^3$

$[+\, \gamma + g \to \psi + g]$

Notes:
All the computations were done with HELAC-ONIA. The scale and mass uncertainties are shown by the hatched and solid bands. **H.S. Shao, CPC198 (2016) 238**; See also `https://nloaccess.in2p3.fr`

[The quark and antiquark attached to the ellipsis are taken as on-shell and their relative velocity v is set to zero.]

NLO⋆ only contains the real-emission contributions with an IR cut-off and is expected to account for the leading P_T contributions at NLO (P_T^{-6}). It has been succesfully checked against full NLO computations for $P_T > 3$ GeV.

Comparison to the latest HERA data by H1

C.Flore, JP Lansberg, H.S. Shao, YY, PLB 811 (2020) 135926

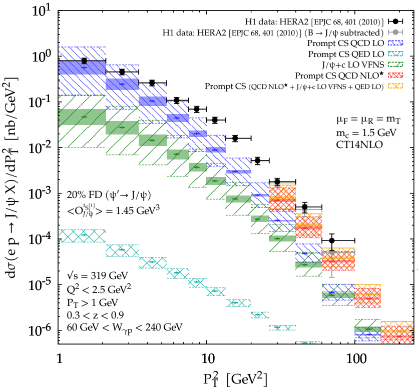

Comparison to the latest HERA data by H1

C.Flore, JP Lansberg, H.S. Shao, YY, PLB 811 (2020) 135926

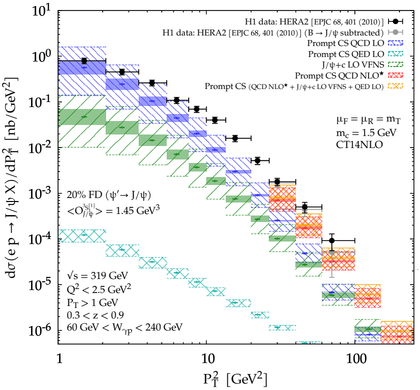

- LO QCD : OK at low P_T

Comparison to the latest HERA data by H1

C.Flore, JP Lansberg, H.S. Shao, YY, PLB 811 (2020) 135926

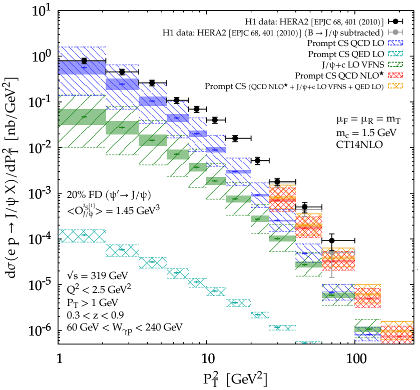

- LO QCD : OK at low P_T
- LO QED small but much harder

Comparison to the latest HERA data by H1

C.Flore, JP Lansberg, H.S. Shao, YY, PLB 811 (2020) 135926

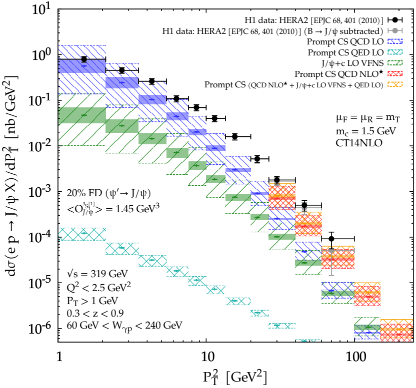

- LO QCD : OK at low P_T
- LO QED small but much harder
- J/ψ+charm: matter at high P_T

Comparison to the latest HERA data by H1

C.Flore, JP Lansberg, H.S. Shao, YY, PLB 811 (2020) 135926

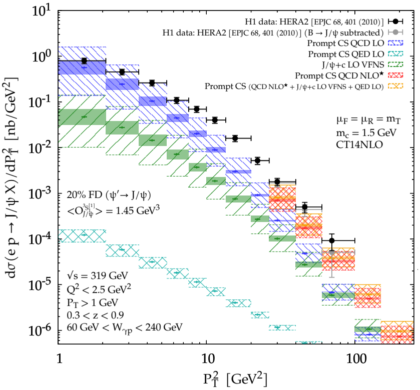

- LO QCD : OK at low P_T
- LO QED small but much harder
- J/ψ+charm: matter at high P_T
- NLO$^{(\star)}$ close the data, the overall sum nearly agrees with them

Comparison to the latest HERA data by H1

C.Flore, JP Lansberg, H.S. Shao, YY, PLB 811 (2020) 135926

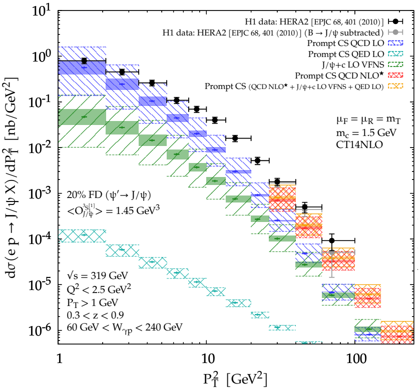

- LO QCD : OK at low P_T
- LO QED small but much harder
- J/ψ+charm: matter at high P_T
- NLO$^{(\star)}$ close the data, the overall sum nearly agrees with them
- Agreement with the last bin when the expected $B \to J/\psi$ feed down (in gray) is subtracted

Comparison to the latest HERA data by H1

C.Flore, JP Lansberg, H.S. Shao, YY, PLB 811 (2020) 135926

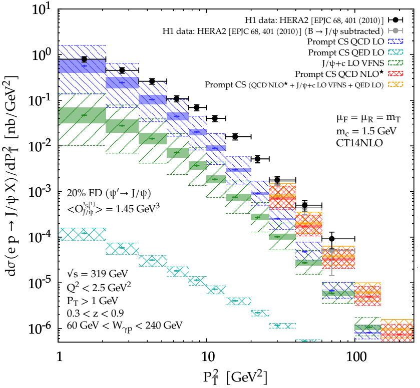

- LO QCD : OK at low P_T
- LO QED small but much harder
- J/ψ+charm: matter at high P_T
- NLO$^{(\star)}$ close the data, the overall sum nearly agrees with them
- Agreement with the last bin when the expected $B \to J/\psi$ feed down (in gray) is subtracted

The CSM up to $\alpha\alpha_s^3$ reproduces photoproduction at HERA

$\rightarrow$ we will restrict to CSM for our EIC predictions

Part III

Photoproduction at mid and high P_T at the Electron-Ion Collider

Predictions for the EIC : $J/\psi + X$

C. Flore, J.P. Lansberg, H.S. Shao, YY, PLB 811 (2020) 135926

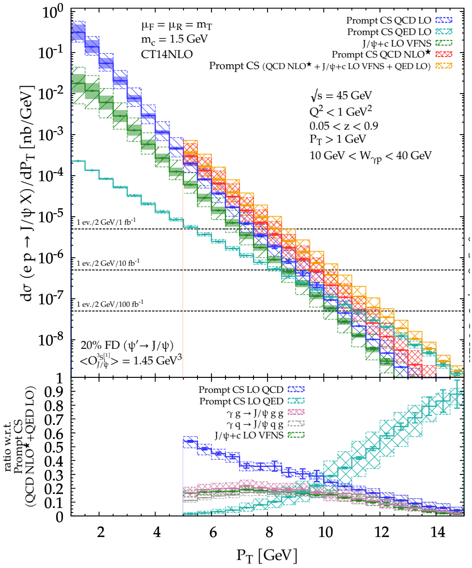

- At $\sqrt{s_{ep}} = 45$ GeV, one gets into valence region

Predictions for the EIC : $J/\psi + X$

C. Flore, J.P. Lansberg, H.S. Shao, YY, PLB 811 (2020) 135926

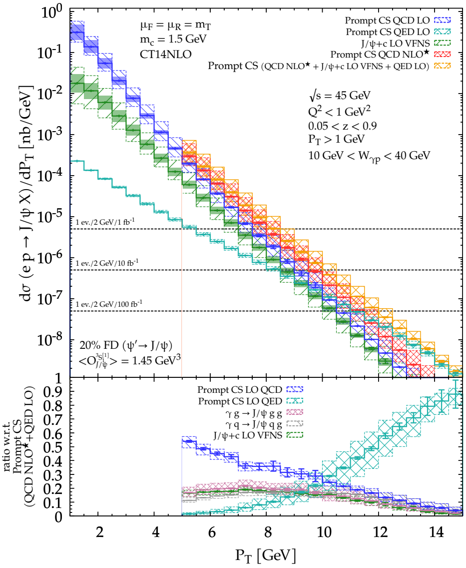

- At $\sqrt{s_{ep}} = 45$ GeV, one gets into valence region
- Yield steeply falling with P_T
- Yield can be measured up to $P_T \sim 11$ GeV with $\mathcal{L} = 100$ fb^{-1}

  [using both *ee* and $\mu\mu$ decay channels and $\varepsilon_{J/\psi} \simeq 80\%$]

Predictions for the EIC : $J/\psi + X$

C. Flore, J.P. Lansberg, H.S. Shao, YY, PLB 811 (2020) 135926

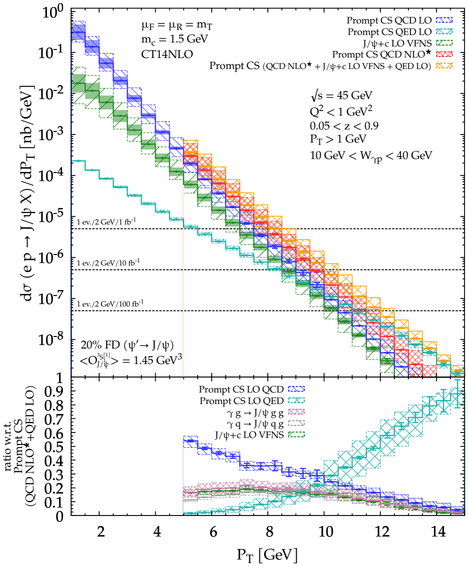

- At $\sqrt{s_{ep}} = 45$ GeV, one gets into valence region
- Yield steeply falling with P_T
- Yield can be measured up to $P_T \sim 11$ GeV with $\mathcal{L} = 100$ fb^{-1}
  [using both *ee* and $\mu\mu$ decay channels and $\varepsilon_{J/\psi} \simeq 80\%$]
- QED contribution leading at the largest reachable P_T
- photon-quark fusion contributes more than 30 % for $P_T > 8$ GeV
- contamination for probing gluon PDFs

Predictions for the EIC : $J/\psi + X$

C. Flore, J.P. Lansberg, H.S. Shao, YY, PLB 811 (2020) 135926

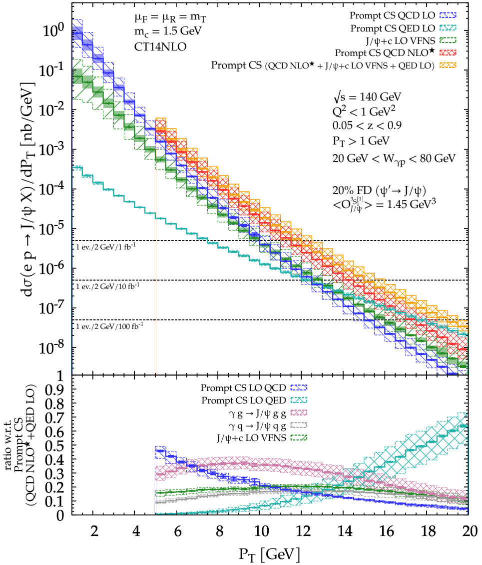

- At $\sqrt{s_{ep}} = 140$ GeV, larger P_T range up to approx. 18 GeV

Predictions for the EIC : $J/\psi + X$

C. Flore, J.P. Lansberg, H.S. Shao, YY, PLB 811 (2020) 135926

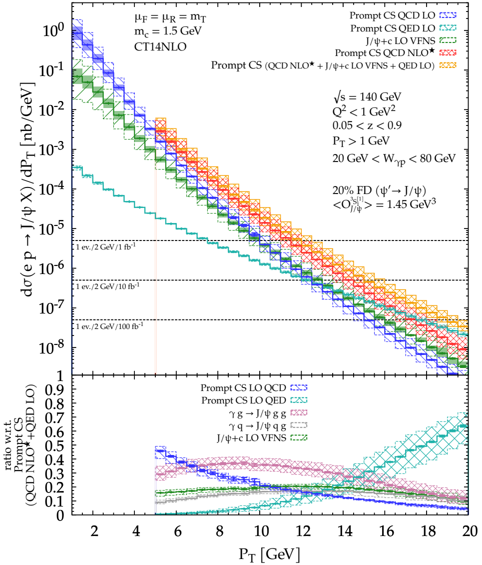

- At $\sqrt{s_{ep}} = 140$ GeV, larger P_T range up to approx. 18 GeV
- QED contribution also leading at the largest reachable P_T
- photon-gluon fusion contributions dominant up to approx. 15 GeV
- potential probe of gluon PDFs

Predictions for the EIC : $J/\psi + X$

C. Flore, J.P. Lansberg, H.S. Shao, YY, PLB 811 (2020) 135926

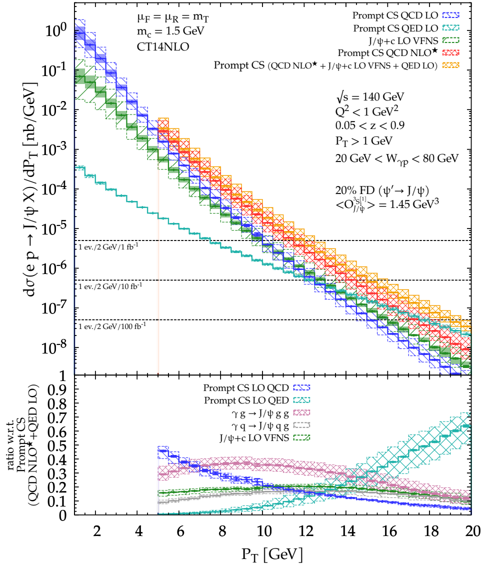

- At $\sqrt{s_{ep}} = 140$ GeV, larger P_T range up to approx. 18 GeV
- QED contribution also leading at the largest reachable P_T
- photon-gluon fusion contributions dominant up to approx. 15 GeV
- potential probe of gluon PDFs
- $J/\psi + 2$ hard partons [*i.e.* $J/\psi + \{gg, qg, c\bar{c}\}$] dominant for $P_T \sim 8 - 15$ GeV

Predictions for the EIC : $J/\psi + X$

C. Flore, J.P. Lansberg, H.S. Shao, YY, PLB 811 (2020) 135926

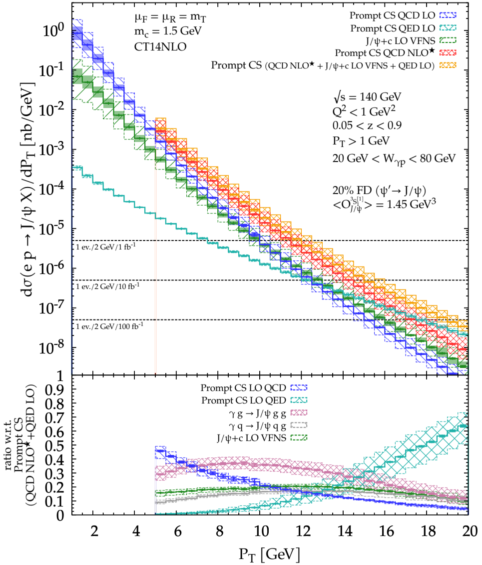

- At $\sqrt{s_{ep}} = 140$ GeV, larger P_T range up to approx. 18 GeV
- QED contribution also leading at the largest reachable P_T
- photon-gluon fusion contributions dominant up to approx. 15 GeV
- potential probe of gluon PDFs
- $J/\psi + 2$ hard partons [*i.e.* $J/\psi + \{gg, qg, c\bar{c}\}$] dominant for $P_T \sim 8 - 15$ GeV
- It could lead to the observation of $J/\psi + 2$ jets with moderate $P_T^{\rm jet}$

Predictions for the EIC : $J/\psi + X$

C. Flore, J.P. Lansberg, H.S. Shao, YY, PLB 811 (2020) 135926

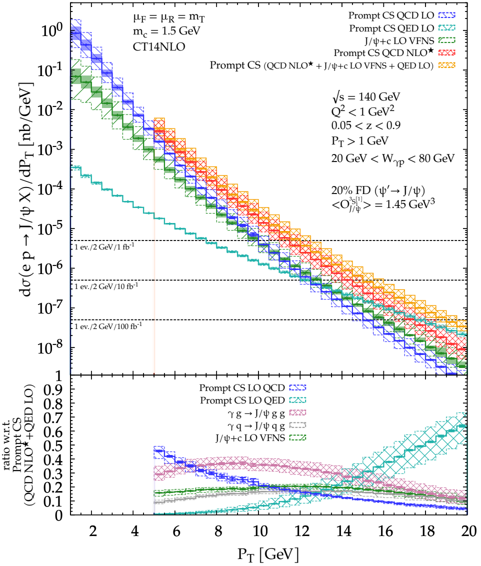

- At $\sqrt{s_{ep}} = 140$ GeV, larger P_T range up to approx. 18 GeV
- QED contribution also leading at the largest reachable P_T
- photon-gluon fusion contributions dominant up to approx. 15 GeV
- potential probe of gluon PDFs
- $J/\psi + 2$ hard partons [*i.e.* $J/\psi + \{gg, qg, c\bar{c}\}$] dominant for $P_T \sim 8 - 15$ GeV
- It could lead to the observation of $J/\psi + 2$ jets with moderate $P_T^{\rm jet}$

Predictions for the EIC : $J/\psi + X$

C. Flore, J.P. Lansberg, H.S. Shao, YY, PLB 811 (2020) 135926

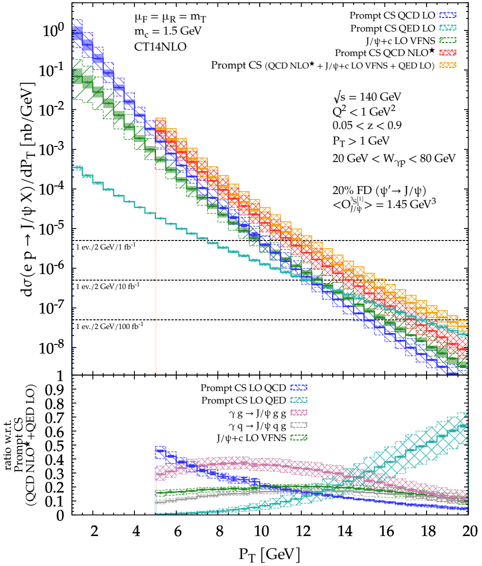

- At $\sqrt{s_{ep}} = 140$ GeV, larger P_T range up to approx. 18 GeV
- QED contribution also leading at the largest reachable P_T
- photon-gluon fusion contributions dominant up to approx. 15 GeV
- potential probe of gluon PDFs
- $J/\psi + 2$ hard partons [*i.e.* $J/\psi + \{gg, qg, c\bar{c}\}$] dominant for $P_T \sim 8 - 15$ GeV
- It could lead to the observation of $J/\psi + 2$ jets with moderate $P_T^{\rm jet}$

Part IV

J/ψ+charm associated production at the EIC

J/ψ+charm associated production at the EIC

C. Flore, J.P. Lansberg, H.S. Shao, YY, PLB 811 (2020) 135926

J/ψ+charm associated production at the EIC

C. Flore, J.P. Lansberg, H.S. Shao, YY, PLB 811 (2020) 135926

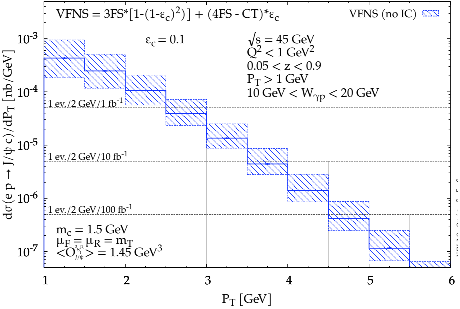

- Same LO VFNS computation previously shown in green except for the charm-detection efficiency ϵ_c: $\sigma^{VFNS} = \sigma^{3FS} \times (1-(1-\epsilon)^2) + (\sigma^{4FS} - \sigma^{CT}) \times \epsilon$
- At $\sqrt{s_{ep}} = 45$ GeV, yield limited to low P_T even with $\mathcal{L} = 100$ fb^{-1}
- But it is clearly observable if $\epsilon_c = 0.1$ with $\mathcal{O}(500, 50, 5)$ events for $\mathcal{L} = (100, 10, 1)$ fb^{-1}

J/ψ+charm associated production at the EIC

C. Flore, J.P. Lansberg, H.S. Shao, YY, PLB 811 (2020) 135926

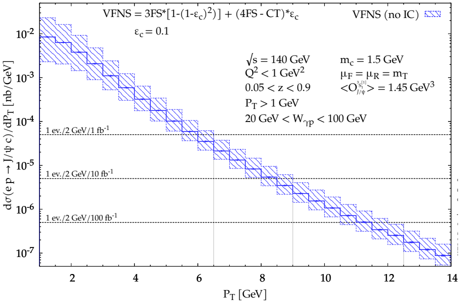

- Same LO VFNS computation previously shown in green except for the charm-detection efficiency ϵ_c: $\sigma^{VFNS} = \sigma^{3FS} \times (1-(1-\epsilon)^2) + (\sigma^{4FS} - \sigma^{CT}) \times \epsilon$
- At $\sqrt{s_{ep}} = 45$ GeV, yield limited to low P_T even with $\mathcal{L} = 100$ fb^{-1}
- But it is clearly observable if $\epsilon_c = 0.1$ with $\mathcal{O}(500, 50, 5)$ events for $\mathcal{L} = (100, 10, 1)$ fb^{-1}
- At $\sqrt{s_{ep}} = 140$ GeV, P_T range up to 10 GeV with up to thousands of events with $\mathcal{L} = 100$ fb^{-1}
- Could be observed via charm jet

J/ψ+charm associated production at the EIC

C. Flore, J.P. Lansberg, H.S. Shao, YY, PLB 811 (2020) 135926

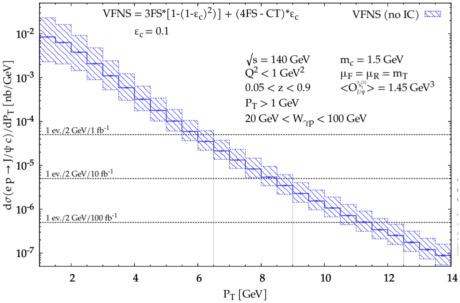

- Same LO VFNS computation previously shown in green except for the charm-detection efficiency ϵ_c: $\sigma^{VFNS} = \sigma^{3FS} \times (1-(1-\epsilon)^2) + (\sigma^{4FS} - \sigma^{CT}) \times \epsilon$
- At $\sqrt{s_{ep}} = 45$ GeV, yield limited to low P_T even with $\mathcal{L} = 100$ fb^{-1}
- But it is clearly observable if $\epsilon_c = 0.1$ with $\mathcal{O}(500, 50, 5)$ events for $\mathcal{L} = (100, 10, 1)$ fb^{-1}
- At $\sqrt{s_{ep}} = 140$ GeV, P_T range up to 10 GeV with up to thousands of events with $\mathcal{L} = 100$ fb^{-1}
- Could be observed via charm jet

- 4FS $\gamma c \to J/\psi c$ depend on $c(x)$ and could be enhanced by intrinsic charm

J/ψ+charm associated production at the EIC

C. Flore, J.P. Lansberg, H.S. Shao, YY, PLB 811 (2020) 135926

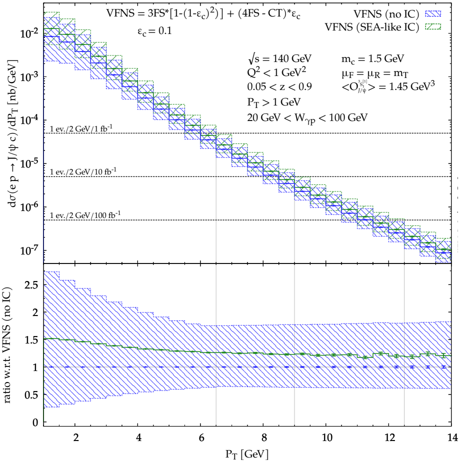

- Same LO VFNS computation previously shown in green except for the charm-detection efficiency ϵ_c: $\sigma^{VFNS} = \sigma^{3FS} \times (1-(1-\epsilon)^2) + (\sigma^{4FS} - \sigma^{CT}) \times \epsilon$
- At $\sqrt{s_{ep}} = 45$ GeV, yield limited to low P_T even with $\mathcal{L} = 100$ fb^{-1}
- But it is clearly observable if $\epsilon_c = 0.1$ with $\mathcal{O}(500, 50, 5)$ events for $\mathcal{L} = (100, 10, 1)$ fb^{-1}
- At $\sqrt{s_{ep}} = 140$ GeV, P_T range up to 10 GeV with up to thousands of events with $\mathcal{L} = 100$ fb^{-1}
- Could be observed via charm jet

- 4FS $\gamma c \to J/\psi c$ depend on $c(x)$ and could be enhanced by intrinsic charm
- Small effect at $\sqrt{s_{ep}} = 140$ GeV [We used IC $c(x)$ encoded in CT14NNLO]

J/ψ+charm associated production at the EIC

C. Flore, J.P. Lansberg, H.S. Shao, YY, PLB 811 (2020) 135926

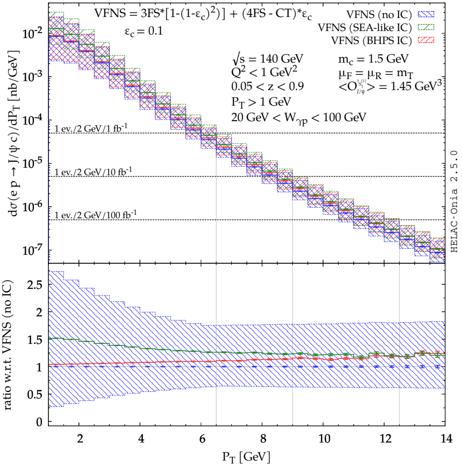

- Same LO VFNS computation previously shown in green except for the charm-detection efficiency ϵ_c: $\sigma^{VFNS} = \sigma^{3FS} \times (1-(1-\epsilon)^2) + (\sigma^{4FS} - \sigma^{CT}) \times \epsilon$
- At $\sqrt{s_{ep}} = 45$ GeV, yield limited to low P_T even with $\mathcal{L} = 100$ fb^{-1}
- But it is clearly observable if $\epsilon_c = 0.1$ with $\mathcal{O}(500, 50, 5)$ events for $\mathcal{L} = (100, 10, 1)$ fb^{-1}
- At $\sqrt{s_{ep}} = 140$ GeV, P_T range up to 10 GeV with up to thousands of events with $\mathcal{L} = 100$ fb^{-1}
- Could be observed via charm jet

- 4FS $\gamma c \to J/\psi c$ depend on $c(x)$ and could be enhanced by intrinsic charm
- Small effect at $\sqrt{s_{ep}} = 140$ GeV [We used IC $c(x)$ encoded in CT14NNLO]

J/ψ+charm associated production at the EIC

C. Flore, J.P. Lansberg, H.S. Shao, YY, PLB 811 (2020) 135926

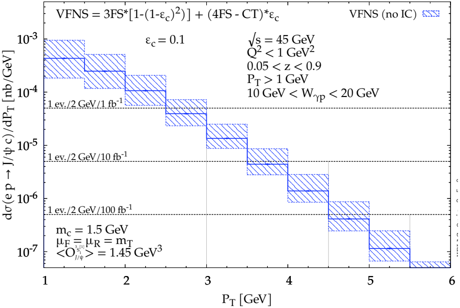

- Same LO VFNS computation previously shown in green except for the charm-detection efficiency ϵ_c: $\sigma^{VFNS} = \sigma^{3FS} \times (1-(1-\epsilon)^2) + (\sigma^{4FS} - \sigma^{CT}) \times \epsilon$
- At $\sqrt{s_{ep}} = 45$ GeV, yield limited to low P_T even with $\mathcal{L} = 100$ fb^{-1}
- But it is clearly observable if $\epsilon_c = 0.1$ with $\mathcal{O}(500, 50, 5)$ events for $\mathcal{L} = (100, 10, 1)$ fb^{-1}
- At $\sqrt{s_{ep}} = 140$ GeV, P_T range up to 10 GeV with up to thousands of events with $\mathcal{L} = 100$ fb^{-1}
- Could be observed via charm jet

- 4FS $\gamma c \to J/\psi c$ depend on $c(x)$ and could be enhanced by intrinsic charm
- Small effect at $\sqrt{s_{ep}} = 140$ GeV [We used IC $c(x)$ encoded in CT14NNLO]
- Measurable effect at $\sqrt{s_{ep}} = 45$ GeV

J/ψ+charm associated production at the EIC

C. Flore, J.P. Lansberg, H.S. Shao, YY, PLB 811 (2020) 135926

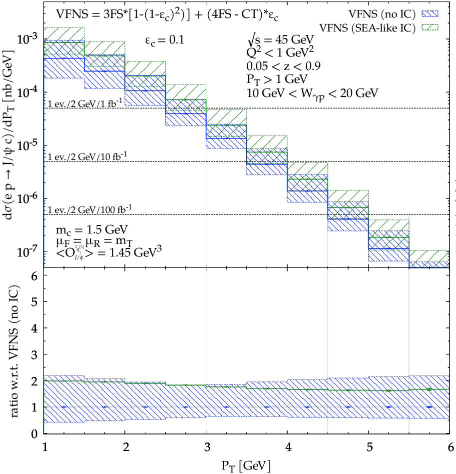

- Same LO VFNS computation previously shown in green except for the charm-detection efficiency ϵ_c: $\sigma^{VFNS} = \sigma^{3FS} \times (1-(1-\epsilon)^2) + (\sigma^{4FS} - \sigma^{CT}) \times \epsilon$
- At $\sqrt{s_{ep}} = 45$ GeV, yield limited to low P_T even with $\mathcal{L} = 100$ fb^{-1}
- But it is clearly observable if $\epsilon_c = 0.1$ with $\mathcal{O}(500, 50, 5)$ events for $\mathcal{L} = (100, 10, 1)$ fb^{-1}
- At $\sqrt{s_{ep}} = 140$ GeV, P_T range up to 10 GeV with up to thousands of events with $\mathcal{L} = 100$ fb^{-1}
- Could be observed via charm jet

- 4FS $\gamma c \to J/\psi c$ depend on $c(x)$ and could be enhanced by intrinsic charm
- Small effect at $\sqrt{s_{ep}} = 140$ GeV [We used IC $c(x)$ encoded in CT14NNLO]
- Measurable effect at $\sqrt{s_{ep}} = 45$ GeV

J/ψ+charm associated production at the EIC

C. Flore, J.P. Lansberg, H.S. Shao, YY, PLB 811 (2020) 135926

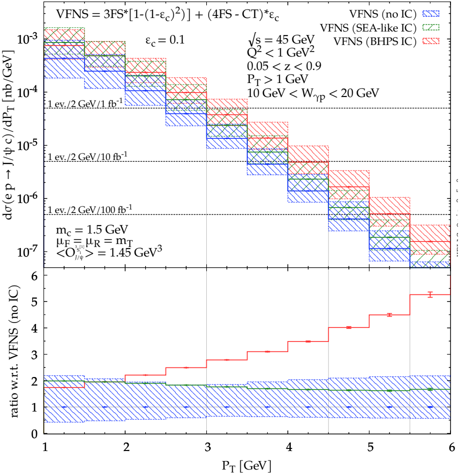

- Same LO VFNS computation previously shown in green except for the charm-detection efficiency ϵ_c: $\sigma^{VFNS} = \sigma^{3FS} \times (1-(1-\epsilon)^2) + (\sigma^{4FS} - \sigma^{CT}) \times \epsilon$
- At $\sqrt{s_{ep}} = 45$ GeV, yield limited to low P_T even with $\mathcal{L} = 100$ fb^{-1}
- But it is clearly observable if $\epsilon_c = 0.1$ with $\mathcal{O}(500, 50, 5)$ events for $\mathcal{L} = (100, 10, 1)$ fb^{-1}
- At $\sqrt{s_{ep}} = 140$ GeV, P_T range up to 10 GeV with up to thousands of events with $\mathcal{L} = 100$ fb^{-1}
- Could be observed via charm jet

- 4FS $\gamma c \to J/\psi c$ depend on $c(x)$ and could be enhanced by intrinsic charm
- Small effect at $\sqrt{s_{ep}} = 140$ GeV [We used IC $c(x)$ encoded in CT14NNLO]
- Measurable effect at $\sqrt{s_{ep}} = 45$ GeV: BHPS valence-like peak visible !

Part V

Study of the impact of the NLO corrections to P_T-integrated cross section

Negative partonic limit

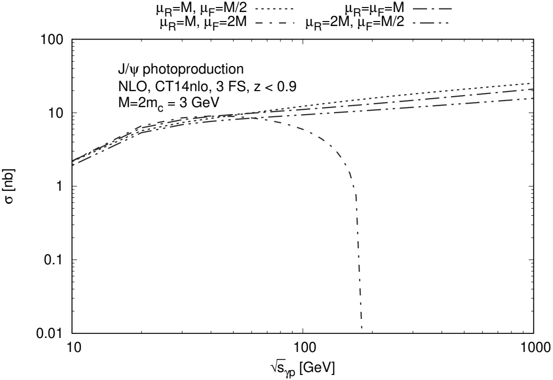

- The partonic high-energy limit:
  $\lim_{\hat{s}\to\infty}(\hat{\sigma}^{NLO}) \sim \frac{\alpha_s}{\pi}\hat{\sigma}_0^{LO}(\log\frac{M^2}{\mu_F^2} + \hat{A});$

Negative partonic limit

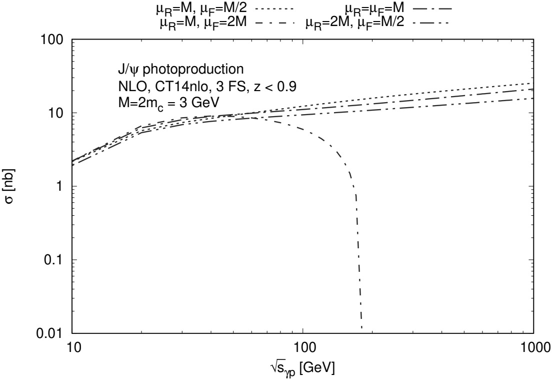

- The partonic high-energy limit: $\lim_{\hat{s}\to\infty}(\hat{\sigma}^{NLO}) \sim \frac{\alpha_s}{\pi}\hat{\sigma}_0^{LO}(\log\frac{M^2}{\mu_F^2}+\hat{A})$;
- large $\mu_F \to \sigma < 0$.

J/ψ: μ_R & μ_F choice

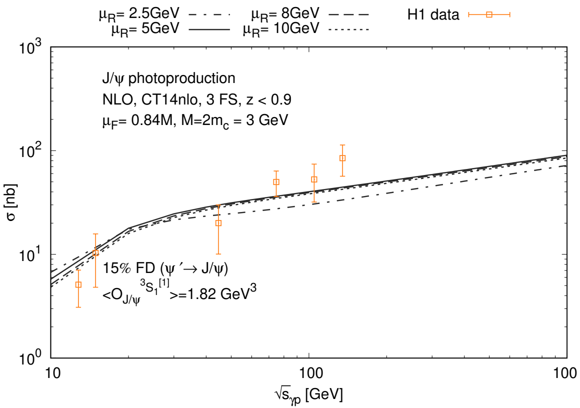

- The choice of factorisation scale to avoid possible negative hadronic cross-section: $\hat{\mu}_F = 0.84M$ (J.P. Lansberg, M.A. Ozcelik: Eur.Phys.J.C 81 (2021) 6, 497;)

J/ψ: μ_R & μ_F choice

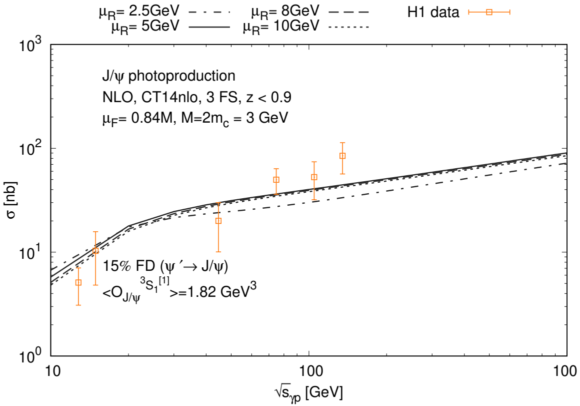

- The choice of factorisation scale to avoid possible negative hadronic cross-section: $\hat{\mu}_F = 0.84M$ (J.P. Lansberg, M.A. Ozcelik: Eur.Phys.J.C 81 (2021) 6, 497;)
- The natural scale in this case is not 3GeV, rather $\sim$ 5GeV ($\hat{s}$ for $\gamma g \to J/\psi g$): $\mu_R = [2.5; 10]GeV$

J/ψ: CT14nlo PDF uncertainties of $\sigma(\sqrt{s_{\gamma p}})$

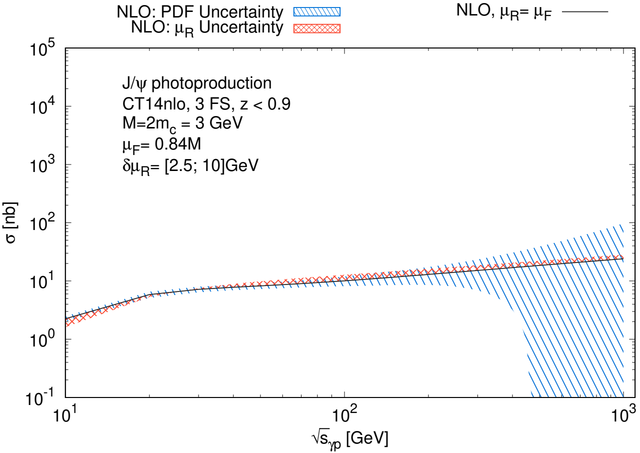

Potential to improve PDFs.

J/ψ: CT14nlo PDF uncertainties for $d\sigma/dz$

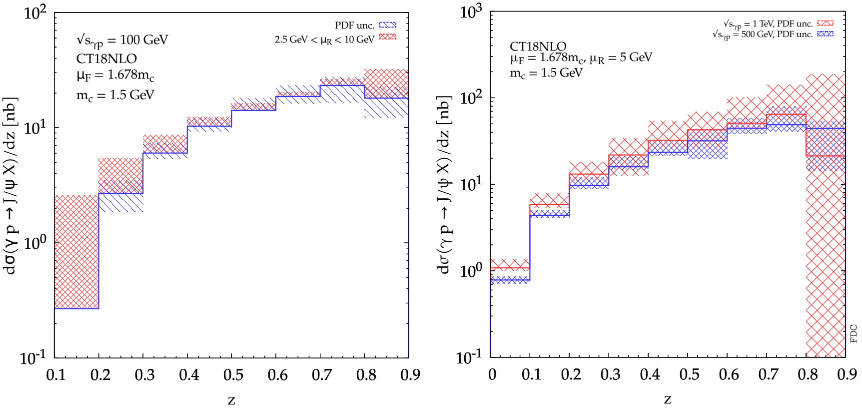

- We can improve PDFs in the region with low x, which corresponds to large z.
- PDF uncertainties are increasing with the growth of CM energy.

Υ photoproduction

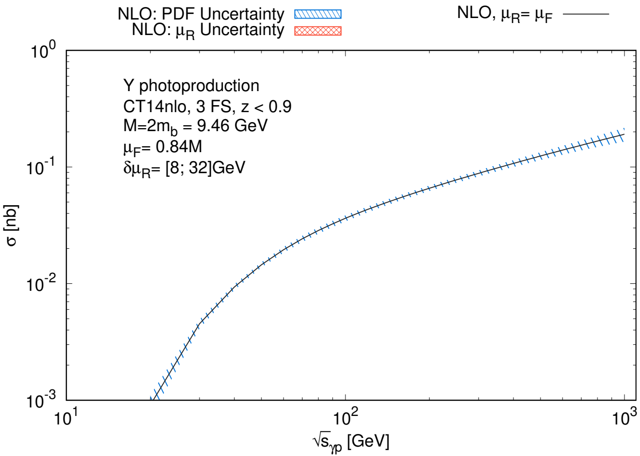

- For Υ we can improve PDFs in the whole range of CM energy.

NB: μ_R uncertainties are not visible.

Conclusions

- For quarkonium production, QCD corrections with P_T-enhanced topologies are known to be important: we have revisited J/ψ photoproduction at HERA

Conclusions

- For quarkonium production, QCD corrections with P_T-enhanced topologies are known to be important: we have revisited J/ψ photoproduction at HERA
- CSM can describe the latest HERA photoproduction data

Conclusions

- For quarkonium production, QCD corrections with P_T-enhanced topologies are known to be important: we have revisited J/ψ photoproduction at HERA
- CSM can describe the latest HERA photoproduction data
- I have presented the QCD-correction study to inclusive J/ψ photoproduction at the EIC

Conclusions

- For quarkonium production, QCD corrections with P_T-enhanced topologies are known to be important: we have revisited J/ψ photoproduction at HERA
- CSM can describe the latest HERA photoproduction data
- I have presented the QCD-correction study to inclusive J/ψ photoproduction at the EIC
- $\sqrt{s_{ep}} = 140$ GeV,
  - gamma-quark QED contribution leading at high P_T
  - gluon-fusion mostly dominant
  - J/ψ+charm jet accessible
  - $J/\psi + 2$ jets accessible

Conclusions

- For quarkonium production, QCD corrections with P_T-enhanced topologies are known to be important: we have revisited J/ψ photoproduction at HERA
- CSM can describe the latest HERA photoproduction data
- I have presented the QCD-correction study to inclusive J/ψ photoproduction at the EIC
- $\sqrt{s_{ep}} = 140$ GeV,
  - gamma-quark QED contribution leading at high P_T
  - gluon-fusion mostly dominant
  - J/ψ+charm jet accessible
  - $J/\psi + 2$ jets accessible
- $\sqrt{s_{ep}} = 45$ GeV,
  - gamma-quark QED contribution leading at high P_T
  - J/ψ+charm sensitive to charm PDFs

Conclusions

- For quarkonium production, QCD corrections with P_T-enhanced topologies are known to be important: we have revisited J/ψ photoproduction at HERA
- CSM can describe the latest HERA photoproduction data
- I have presented the QCD-correction study to inclusive J/ψ photoproduction at the EIC
- $\sqrt{s_{ep}} = 140$ GeV,
  - gamma-quark QED contribution leading at high P_T
  - gluon-fusion mostly dominant
  - J/ψ+charm jet accessible
  - $J/\psi + 2$ jets accessible
- $\sqrt{s_{ep}} = 45$ GeV,
  - gamma-quark QED contribution leading at high P_T
  - J/ψ+charm sensitive to charm PDFs
- Potential to improve PDFs using J/ψ & Υ photoproduction.

Conclusions

- For quarkonium production, QCD corrections with P_T-enhanced topologies are known to be important: we have revisited J/ψ photoproduction at HERA
- CSM can describe the latest HERA photoproduction data
- I have presented the QCD-correction study to inclusive J/ψ photoproduction at the EIC
- $\sqrt{s_{ep}} = 140$ GeV,
  - gamma-quark QED contribution leading at high P_T
  - gluon-fusion mostly dominant
  - J/ψ+charm jet accessible
  - $J/\psi + 2$ jets accessible
- $\sqrt{s_{ep}} = 45$ GeV,
  - gamma-quark QED contribution leading at high P_T
  - J/ψ+charm sensitive to charm PDFs
- Potential to improve PDFs using J/ψ & Υ photoproduction.
- To avoid negative σ^{NLO} we have used $\hat{\mu}_F$ scale prescriptions and have shown that it works.

Conclusions

- For quarkonium production, QCD corrections with P_T-enhanced topologies are known to be important: we have revisited J/ψ photoproduction at HERA
- CSM can describe the latest HERA photoproduction data
- I have presented the QCD-correction study to inclusive J/ψ photoproduction at the EIC
- $\sqrt{s_{ep}} = 140$ GeV,
  - gamma-quark QED contribution leading at high P_T
  - gluon-fusion mostly dominant
  - J/ψ+charm jet accessible
  - $J/\psi + 2$ jets accessible
- $\sqrt{s_{ep}} = 45$ GeV,
  - gamma-quark QED contribution leading at high P_T
  - J/ψ+charm sensitive to charm PDFs
- Potential to improve PDFs using J/ψ & Υ photoproduction.
- To avoid negative σ^{NLO} we have used $\hat{\mu}_F$ scale prescriptions and have shown that it works.

Thank you for attention!